Spectrochimica Acta Part A: Molecular and Biomolecular Spectroscopy 136 (2015) 1710–1717

Contents lists available at ScienceDirect

Spectrochimica Acta Part A: Molecular and Biomolecular Spectroscopy

journal homepage: www.elsevier.com/locate/saa

Spectral, morphological and antibacterial studies of β-cyclodextrin stabilized silver – Chitosan nanocomposites

N. Punitha [a,*], P.S. Ramesh [b], D. Geetha [c]

[a] Department of Physics, St. Joseph's College of Engineering, Chennai 600119, India
[b] Department of Physics (DDE Wings), Annamalai University, Annamalai Nagar 608002, India
[c] Department of Physics, Annamalai University, Annamalai Nagar 608002, India

HIGHLIGHTS

- Simple, effective and eco-friendly method.
- The silver nanocomposites were crystalline nature and shows good stability.
- Functionalized Ag nanocomposites exhibit enhanced biological activity.

GRAPHICAL ABSTRACT

Formation of β-CD stabilized Ag-Cts NCs.

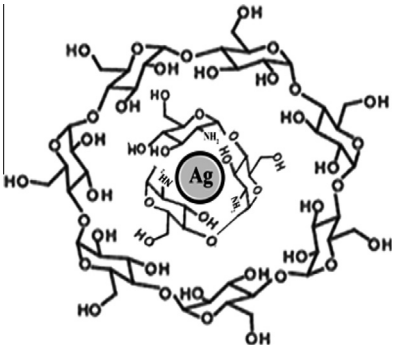

ARTICLE INFO

Article history:
Received 10 August 2014
Received in revised form 5 October 2014
Accepted 19 October 2014
Available online 31 October 2014

Keywords:
Silver nanocomposite
Biodegradable stabilizer
Stability
Antibacterial activity

ABSTRACT

The aim of the study is to investigate the antibacterial properties and characterization of β-cyclodextrin (β-CD) stabilized silver – chitosan nanocomposite (Ag-Cts NCs). An effective and eco-friendly technique for the synthesis of Ag-Cts NCs in the presence of a strong stabilizing agent β-CD is described. The well formed nanocomposites were characterized by the Ultraviolet Visible spectroscopy (UV–Vis), X-ray diffraction (XRD), Fourier Transform Infrared Spectroscopy (FT-IR), Photoluminescence spectroscopy (PL), Scanning electron microscope (SEM/EDS), Atomic force microscope (AFM), High resolution transmission electron microscope (HR-TEM) and Zeta potential measurement (ZP). The results confirmed that the poly dispersed Ag-Cts NCs are less than 15 nm in size with spherical shape and show good stability. The antibacterial activity was also investigated and β-CD coated Ag-Cts NCs showed a promising bacterial activity against gram negative *Escherichia coli* (*E. coli*) and gram positive *Staphylococcus aureus* (*S. aureus*) micro-organism.

Introduction

One of the major applications of nanotechnology is in biomedicine. Nanoparticles (NPs) can be engineered as nanoplatforms for effective and targeted delivery of drugs, imaging labels and antibacterial agents by overcoming the many biological, biophysical and biomedical barriers [1–3]. Various stabilizing agents are available to prevent nanoparticles from aggregating as well as to functionalize the particles for the desired applications [4,5]. However, normally used severe reaction conditions and toxic chemicals may not be suitable for biological and biochemical applications [6].

* Corresponding author. Tel.: +91 9788126549.
E-mail address: punithasan@gmail.com (N. Punitha).

http://dx.doi.org/10.1016/j.saa.2014.10.071
1386-1425/

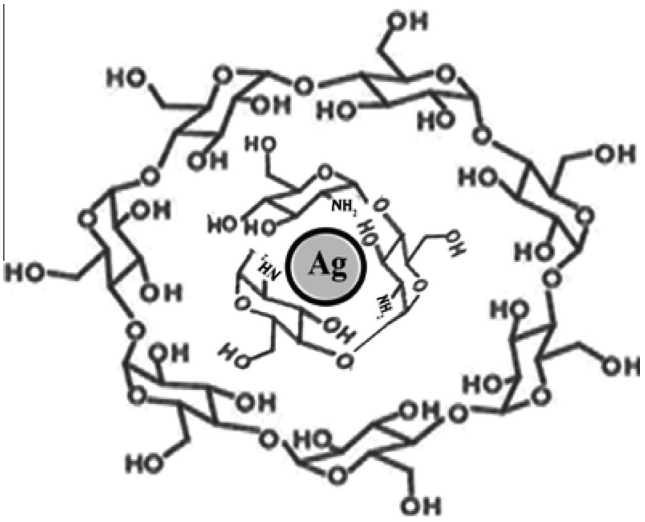

Fig. 1. Formation of β-CD stabilized Ag-Cts NCs.

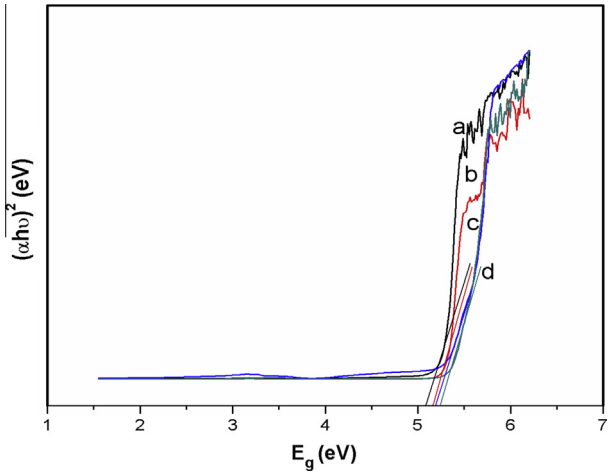

Fig. 3. Optical band gap of (a) Ag-Cts and β-CD stabilized (b) 0.4, (c) 0.8, (d) 1.2 wt% Ag-Cts NCs.

With continued development in the synthesis techniques over the last two decades, most of the metal nanoparticles can now be produced with low cost, renewable, biocompatible, tumor targeting efficacy, non-toxicity and environmental friendly (e.g. green) processes with the help of plant extractions [7–9] and polysaccharide biopolymers, such as starch [10,11], alginate [12,13] and chitosan [14–18]. Nonetheless, due to the tremendous amount of information available, this review will be selectively restricted to the use of biodegradable polymers in the stabilization of metal nanoparticles.

Along with gold, silver is the most extensively used metal for the preparation of NPs with potential biomedical functions [19,20], owing to their exceptional chemical, electronic and plasmonic properties which make them very attractive in molecular sensing [21], diagnosis [22], drug delivery [23], cancer therapy [24,25] and antibacterial action [26–29]. Among antibacterial agents, silver has been employed most extensively to fight infections and control spoilage. It has been known that silver and its compounds have strong inhibitory and bacterial effects as well as a broad spectrum of antimicrobial activities for about 650 types of disease causing microorganisms since ancient times [30]. The recent advancement in nanoparticle research has opened up a new gate way for Ag NPs in the antimicrobial studies.

Table 1
Particle size and Band gap values of various concentrations of β-CD stabilized Ag-Cts NCs.

Samples	Particle size (nm)	Band gap (eV)
Ag-Cts	15.1	5.08
Ag-Cts + β-CD (0.4%)	13.7	5.16
Ag-Cts + β-CD (0.8%)	9.5	5.19
Ag-Cts + β-CD (1.2%)	6.6	5.24

In wet chemical synthesis of metal nanoparticles, an important reactant is stabilizing or capping agents, which function as a barrier to prevent the uncontrolled growth processes. A good choice among these agents (also known as surfactants or stabilizers) is one that involves organic molecules that have a suitable hydrophobic end that binds to the metal NPs covalently and is soluble on the other end. β-CD is a good surfactant that has an ionic tail that aids the solution of the NPs and exhibits columbic repulsion of similar surfactants on the neighboring NPs, which helps dispersion. As

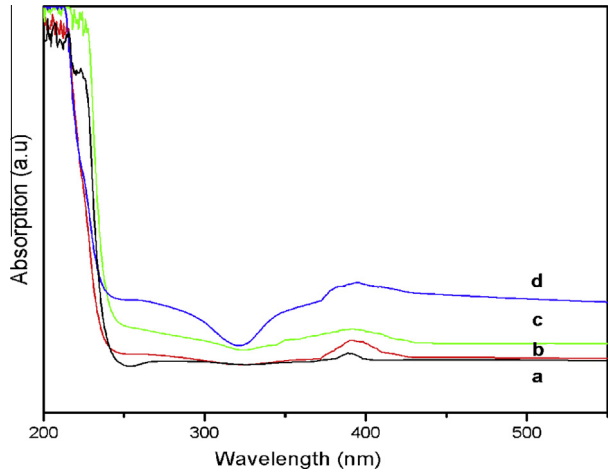

Fig. 2. UV–Vis absorption spectra of (a) Ag-Cts and β-CD stabilized (b) 0.4, (c) 0.8, (d) 1.2 wt% Ag-Cts NCs.

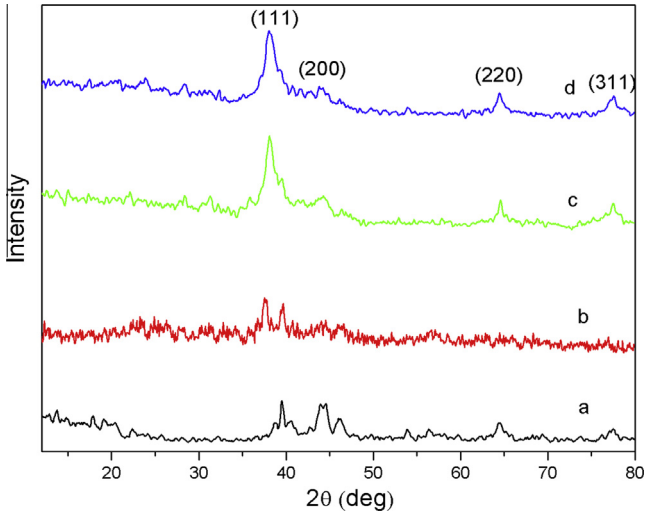

Fig. 4. XRD patterns of (a) Ag-Cts and β-CD stabilized (b) 0.4, (c) 0.8, (d) 1.2 wt% Ag-Cts NCs.

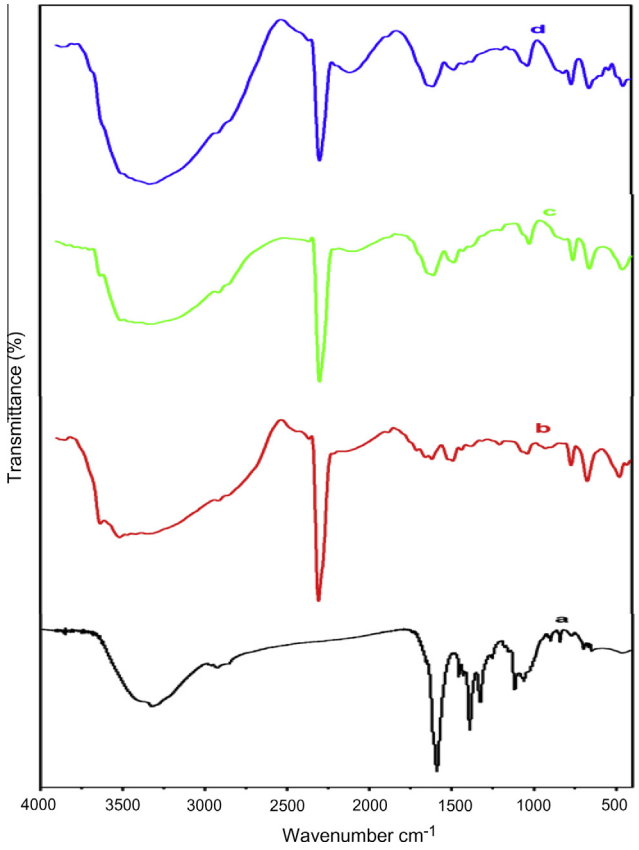

Fig. 5. FT-IR spectra of (a) Ag-Cts and β-CD stabilized (b) 0.4, (c) 0.8, (d) 1.2 wt% Ag-Cts NCs.

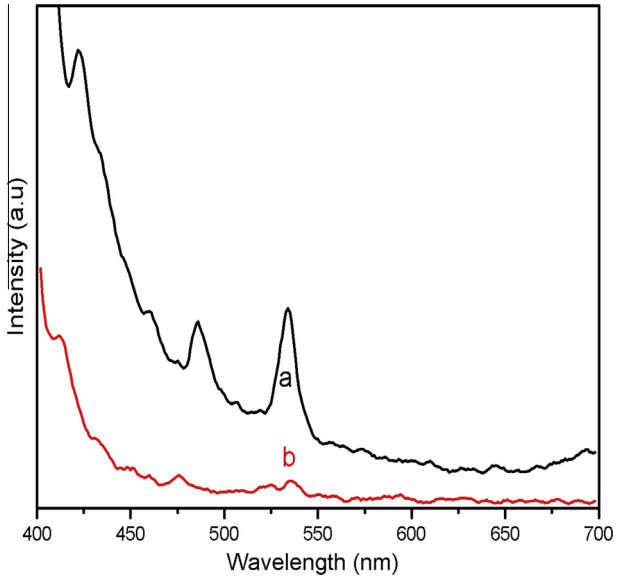

Fig. 6. PL spectra of (a) Ag-Cts and β-CD stabilized (b) 0.8 wt% Ag-Cts NCs.

complexing agents, CDs can be applied to enhance solubility, act as a protection for the smaller guest compounds and selectively remove substances from a given mixture. Among the CDs β-CD is most widely employed due to the ideal cavity diameter of 6–6.5 Å. There have been numerous studies of CDs application as stabilizing agents for various metallic NPs such as Au, Ag and Pt and in which CDs were used as thiolated CD or in some other

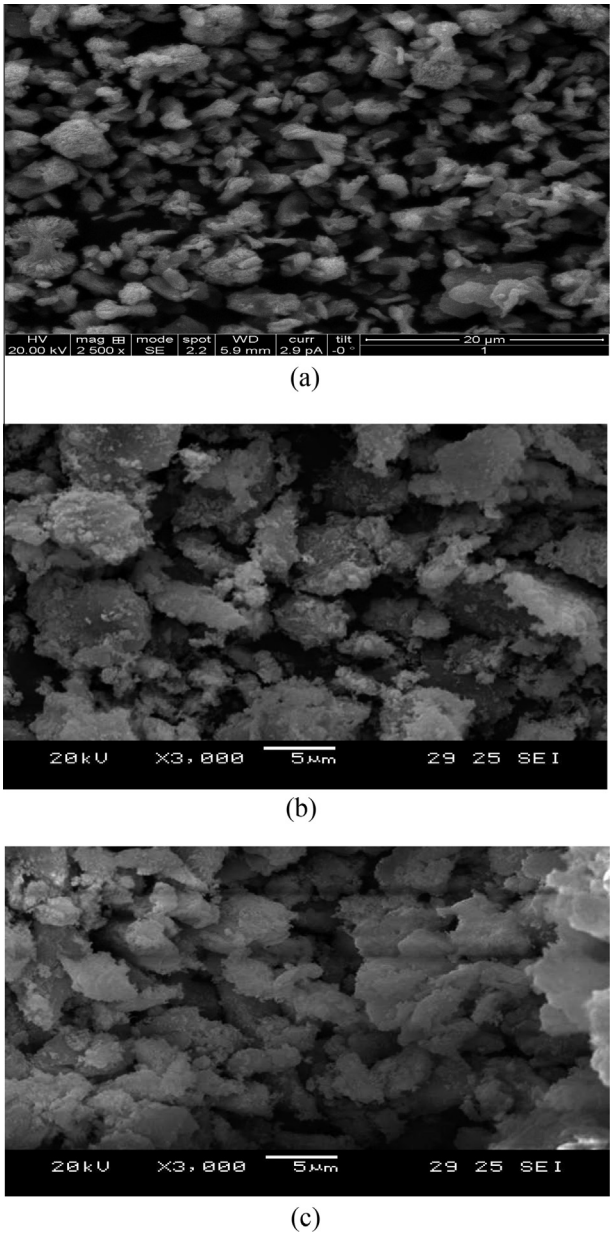

Fig. 7. SEM image of (a) Ag-Cts and β-CD stabilized (b) 0.8, (c) 1.2 wt% Ag-Cts NCs.

modified form for greater attachment of particles [31–35]. In recent studies unmodified CD has been used mainly for its functional group and solubility [36–38].

The NPs can enter the human body through many ways and are likely to cause health issues, if the level exceeds a certain limit. Hence it becomes very important to synthesis NPs through greater and less hazardous methods. One such method for the synthesis of metal nanoparticles is the simple reduction of metal chlorides and nitrates into metal NPs by Cts in the presence of aqueous β-CD which is supposed to be more convenient and environmentally benign (Fig. 1).

Experimental technique

Materials

Silver nitrate ($AgNO_3$) and polymers viz., Chitosan and β-cyclodextrin, were purchased from Sd-fine. All the chemicals were used

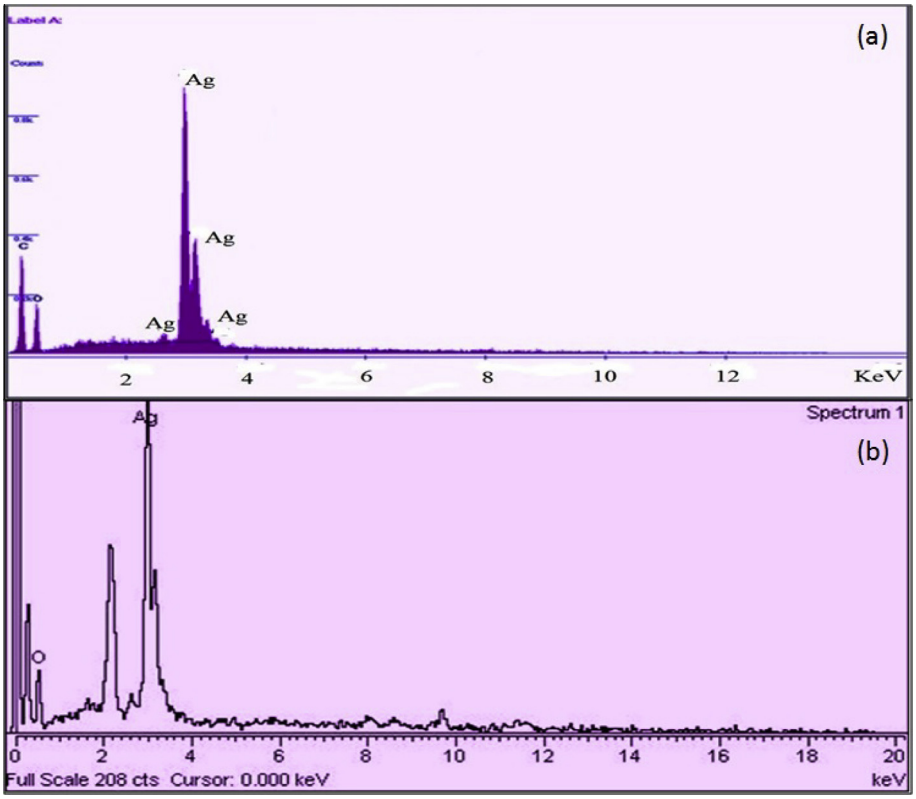

Fig. 8. EDS image of (a) Ag-Cts and (b) β-CD stabilized 0.8 wt% Ag-Cts NCs.

as received, since they were of analytical reagent grade with 99% purity.

Synthesis of silver nanocomposites

The synthesis of β-CD capped Ag NPs was achieved by the simplest and widely used chemical reduction technique [39,40]. The reaction mixture contains 0.1 M of aqueous silver nitrate and sodium citrate solutions. To this mixture 0.5% of aqueous Cts was added. Then, different concentrations of aqueous β-CD (0.4, 0.8 and 1.2 wt%) were added with Ag-Cts solution under the continuous stirring over a 45 min period and kept at 300 °C for 10 min. The transparent colorless solution was converted to the characteristic yellowish-brown color, indicating the formation of silver nanoparticles. The mixture was then allowed to cool at room temperature. Finally, the precipitation formed was collected and washed with ethanol and deionized water several times to remove impurities. Then the samples were dried at 60 °C for 4 h and collected in powder form.

Characterization techniques

UV–Vis absorption spectra were measured using a UV–Visible spectrophotometer (SHIMADZU-UV 1800), employing deionized water as the reference. X-ray powder diffraction (XRD) of the samples was carried out on an XPERT-PRO diffractometer with Cu Ka radiation (l = 0.15406 nm). Fourier transformation infrared (FT-IR) spectrum was recorded by FT-IR spectrometer (NICOLET iS5) ranging from 400 to 4000 cm^{-1}.

The prepared samples were characterized by Scanning electron microscope (SEM/EDS) (JEOL-JSM – 5610 LV) with INCA EDS. The Photoluminescence (PL) emission spectra of the samples were recorded by fluorescence spectrophotometer (Perkin–Elmer LS55) excited at λ_{exc} = 390 nm. Atomic force microscopy (AFM) image of the sample was performed in the air with a digital Instrument AGILENT – NP410A series 5500 AFM in contact mode. The particle size and shape were confirmed using JEOL HRTEM. Zeta potential values were measured using zetasizer Nano ZS Instrument (Malvern Instruments Corporation).

The biological culture was performed using an agar well diffusion method. The gram negative bacteria *E. coli* (ATCC8739) and the gram positive bacteria *Staphylococcus aureus* (ATCC65) were used for measurement of Minimum Inhibitory Concentration (MIC) of β-CD stabilized Ag-Cts NCs. The bacteria were cultured on agar plates and then incubated overnight at 37 °C and the antibacterial effect was determined by the zone of inhibition.

Results and discussion

Optical study (UV–Visible)

The formation of Ag NPs in the polymeric media was determined by using UV–Vis spectroscopy, which was shown on the surface plasmon resonance (SPR) bands. The appearance of a plasmon peak around 392 nm (Fig. 2) in the absence of β-CD is attributed to the formation of spherical Ag-Cts NCs and corresponds to surface plasmon resonance of Ag NPs. When the concentration of β-CD was increased from 0.4 to 1.2 wt%, the blue shift of the SPR band was observed, which strongly suggests a decrease in the particle size. Generally, the SPR bands were influenced by the size, shape, composition and dielectric environment of the prepared nanocomposites [41,42].

Previous studies have shown that, spherical Ag NPs contribute to the absorption band around 400 nm [43]. In this study the addition of β-CD does not show any sharp absorption peak which shows that Ag-Cts NCs were stabilized by β-CD coating, due to which the transition of free electron from the surface is not possible. A minimum

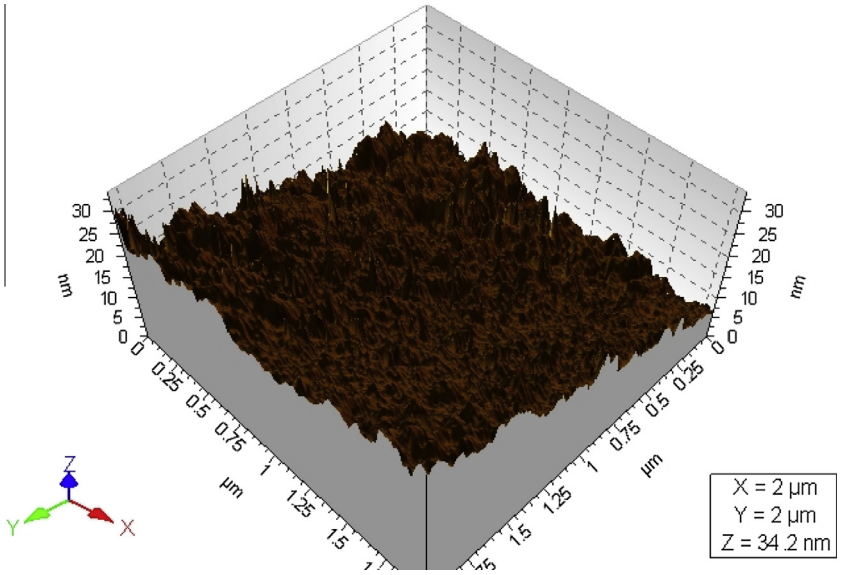

Fig. 9. AFM image of β-CD stabilized 0.8 wt% Ag-Cts NCs.

observed at 330 nm corresponds to the wavelength at which the real and imaginary part of the dielectric function of silver almost vanishes.

Absorption co-efficient (α) associated with the strong absorption region of the sample was calculated from the absorbent (A) and the sample thickness (t) by using the relation,

$$a = 2.303A/t \quad (1)$$

While, the optical band gap of Ag-Cts NCs was calculated using Tauc relation [44].

$$a\ h\upsilon = B(h\upsilon - E_g)^{1/2} \quad (2)$$

where B is a constant, $h\upsilon$ is the energy of the incident photon and the exponent ($n = 1/2$) whose value depends upon the type of transition. The variation of $(\alpha\ h\upsilon)^2$ vs. photon energy hυ for Ag-Cts nanocomposites is shown in (Fig. 3). Allowed direct band gap values of Ag-Cts NCs are calculated and presented in Table 1. These values are comparable to the reported values of Ag synthesized by micro emulsion technique [45]. The increase in the band gap of Ag-Cts NCs with the decrease in particle size is attributed to the quantum confinement effect. [46].

Structural analysis (XRD)

The formation of Ag NPs was also confirmed by powder XRD analysis. The diffraction pattern obtained for various concentrations of the stabilizer (β-CD) in Ag-Cts nanocomposite is reported in (Fig. 4). β-CD is a highly crystalline material with main diffractions at 2θ values viz., 9.1°, 12.5° and 22.7°. From the XRD pattern of the samples, it is evident that the Ag NPs are well crystallized, demonstrating sharp peaks at designated 2θ values Viz., 38°, 44°, 64°, and 77°.

These peaks can be attributed to (111), (200), (220) and (311) crystalline planes of Ag face centered cubic (FCC) lattice [JCPDS: 087-0719] [47]. The intensity of the reflections due to Ag NPs was found to increase with β-CD concentration. However, the interaction of β-CD with Ag-Cts NCs causes a loss of β-CD crystallinity, which was confirmed by the absence of majority of peaks of β-CD in the present pattern. From (Fig. 4a) it can be noticed that some impurities peaks at 2θ values viz., 10.4°, 13.7°, 22.8°, and 28° are observed apart from Ag NPs designated 2θ values. This indicates the crystalline formation of Cts molecule in the absence of β-CD. On addition of β-CD the crystallinity nature of Cts disappears slowly with increasing in concentration of stabilizer. The mean size of Ag NCs was estimated by analyzing the broadening of (111) reflection. Average crystalline sizes for all samples were estimated using the well-known Debye-Scherer's formula [48],

$$D = \frac{k\lambda}{\beta Cos\theta} \quad (3)$$

where λ, β and θ are the X-ray wavelength, the full width half maximum (FWHM) of the diffraction peak and the diffraction angle respectively. The calculated particle sizes are presented in Table 1, which indicate that the size of the particle decreases with the increase of β-CD concentrations.

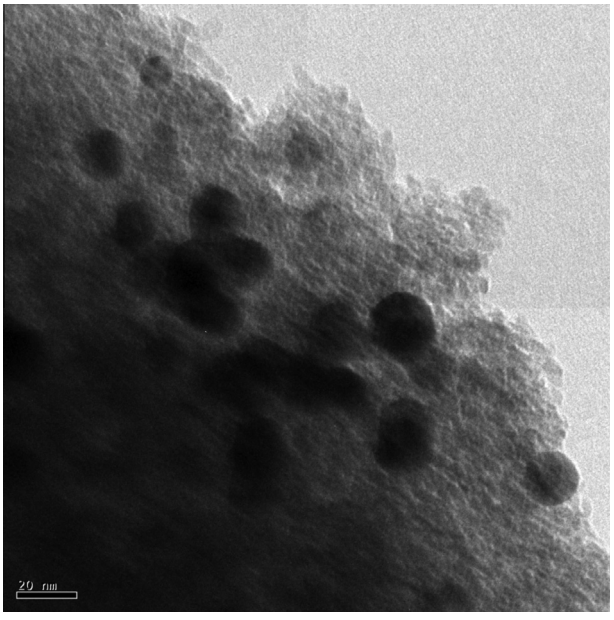

Fig. 10. HR-TEM of β-CD stabilized 0.8 wt% Ag-Cts NCs.

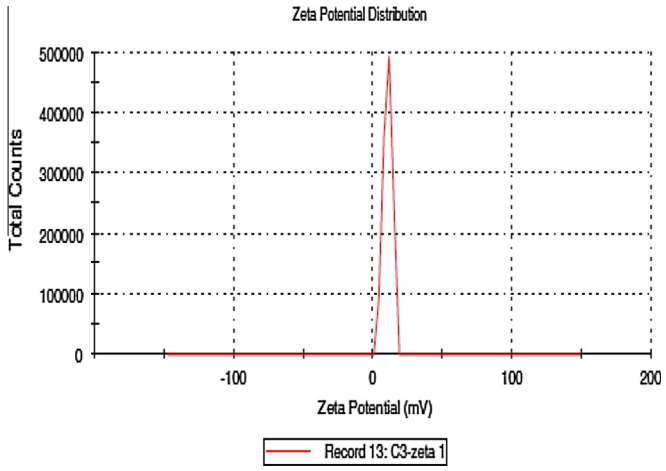

Fig. 11. Zeta potential curve of β-CD stabilized 0.8 wt% Ag-Cts NCs.

Spectral analysis (FT-IR)

FT-IR spectrum measurement was carried out to examine the possible functional groups of Ag-Cts responsible for reduction and β-CD stabilization of the NCs. The spectrum (Fig. 5a) revealed that Ag-Cts NCs spectrum is similar to that of pure silver except the broadening of O—H band at 3400 cm^{-1} which clearly indicates the weaker interaction between the Ag-Cts after the formation of NPs. Once β-CD is introduced few new peaks has been observed in (Fig. 5b–d). The dominant sharp peak at 2357 cm^{-1} and the peak at 1645 cm^{-1} corresponds to N=C vibrations, which clearly confirm the strong interaction between the Cts and carbon atom in β-CD. The broadening of O—H valance vibrations with increase of β-CD concentration further establishes the presence of large quantity of hydroxyl groups. The peak observed at 1515 cm^{-1} and 1330 cm^{-1} corresponds to aliphatic and aromatic C—H stretching vibrations in the complexation [49]. The shifting of O—H stretching, N—H bending and C—O—C band stretching (1045 cm^{-1}) confirmed the interaction of β-CD on Ag-Cts NCs [50,51]. The peaks at 464 cm^{-1}, 542 cm^{-1} and 663 cm^{-1} relate to Ag NPs bonding with oxygen from hydroxyl group [52]. Therefore, the FT-IR spectra showed the existence of Vander – Wall's interaction between the β-CD and Ag NCs in the polymeric media.

Photoluminescence (PL)

The photoluminescence spectra obtained from the Ag-Cts and β-CD stabilized Ag-Cts NCs is depicted in (Fig. 6). The PL emission has been obtained within the visible range 400–600 nm with peak positions at 422 nm, 485 nm and 545 nm. The emission peaks of Cts are characterized by 422 nm and 485 nm which originate from protein residues from the biopolymer and the peak corresponding to 545 nm by the Ag NPs. The addition of β-CD quench the emission of chitosan and silver peaks which may be due to a non-radiative energy transfer mechanism such as charge transfer [53]. This quenching effect could be a consequence of overlap between absorption band of Ag and emission band of biopolymers (Cts/β-CD). Such an effect was observed for Ag-Cts NCs prepared by a green chemical procedure using α glucose as the reducing agent [11]. As the samples were prepared separately under different conditions, the difference in PL emission peaks could be attributed to the different states of agglomeration of growth in particle size. In the case of β-CD capped samples, the observed decrease in PL once again confirms the stability of Ag-Cts NCs as the surface free electrons were partly quenched in the emission process.

Surface morphological studies and stability (SEM/EDS, AFM, HRTEM and Zeta potential)

The micrographs of Ag-Cts and β-CD influenced Ag-Cts mixtures were recorded (Fig. 7). The prepared samples have shown small particles gathered into clusters with spherical and pseudo spherical in shape [54]. The physical mixture appeared as agglomerated β-CD stabilized Ag-Cts NCs and the original morphology disappears so that the complex formation is suggested.

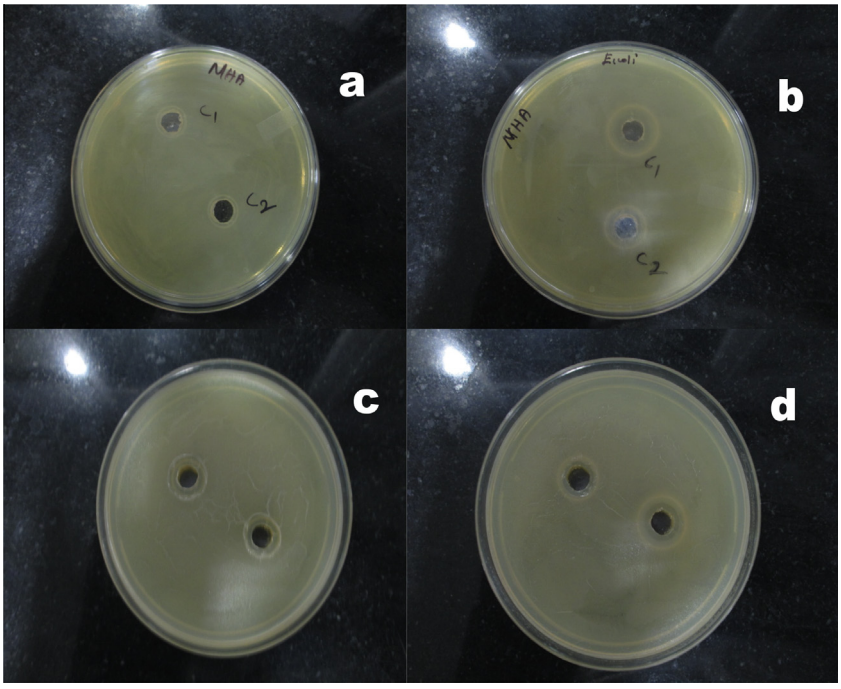

Fig. 12. Antibacterial activity of (a) Ag-Cts, (b) β-CD stabilized Ag-Cts NCs against *E. coli* and (c) Ag-Cts, (d) β-CD stabilized Ag-Cts NCs against *S. aureus*.

The chemical composition of the sample was analyzed by Energy Dispersive Spectroscopy (EDS) (Fig. 8), which confirmed the formation of Ag NPs in the polymeric media [55]. The analysis revealed that the prepared samples exhibit very smooth surface and good crystal structure.

Ag nanocomposites were characterized by AFM for its detail size, morphology and agglomeration of silver. It is the characterization technique for the examination of nanoparticle in contact mode. A topographic image of β-CD (0.8 wt%) stabilized Ag-Cts is presented in (Fig. 9). It is evident that the average size of the particles is observed to be around 12 nm.

HRTEM images of the prepared β-CD (0.8 wt%) stabilized Ag-Cts is shown in (Fig. 10). The Ag-Cts NCs are formed as spherical clusters with smooth surface morphology and poly dispersed [39]. The diameter of the particles is found to be ranging from 10–20 nm. It is established that the particle size and morphology can be modified by employing the reducing and stabilizing agents at proper proportions.

The Zeta potential analysis is a technique for determining the surface charge of NPs. NPs has a surface charge that attracts a thin layer of ions of opposite charge to the nanoparticle surface. Zeta potential is an important tool for understanding the state of nanoparticle surfaces and for predicting the long term stability of the nanocomposite. In the present study the ZP value of β-CD stabilized Ag-Cts NCs was determined as18.6 mV (Fig. 11), while the earlier reported work [56] of the Cts NPs was found to be 32.4 mV.

The decrease of ZP after the stabilization of β-CD may be due to high charge density of β-CD which might deprotonate most of the amino groups of Cts. The above results indicate that β-CD coated Ag-Cts now can have good stability owing to the strong attraction between β-CD and Cts molecules.

Antibacterial activity

The ability of Ag-Cts and β-CD stabilized Ag-Cts NCs to inhibit the growth of tested strains is shown in (Fig. 12). The inhibitory activity was measured based on the diameter of clear inhibition zone. The results of this study suggest that the MIC of Ag NCs (10 μg/ml) was enough to enhance antibacterial activity significantly towards both Gram- negative (*E. coli*) and Gram-positive (*S. aureus*) bacteria [57]. The inhibitory zone was 2 mm and 6 mm for Ag-Cts and β-CD stabilized Ag-Cts NCs respectively. This activity was caused due to Ag NPs and the Ag^+ ions on the surface bind to sulfur- and phosphorus-containing bio-molecules such as DNA or other biological moieties, thereby potentially causing cell damage [58].

Conclusions

In summary, a simple method to synthesis Ag-Cts NCs in the presence of stabilizing agent β-CD, which requires no specific condition, is suggested. The reducing agent (Cts) and stabilizing agent β-CD also played a role of shape modifying agents for the synthesis of Ag NPs. The formation was confirmed by UV–Visible, which shows the characteristic SPR band at 392 nm. The XRD results confirmed Ag NCs possess the face centered cubic structure. The XRD as well as AFM image studies confirmed the size of the Ag NCs. The SEM and HR-TEM images showed that Ag NPs are polydispersed spherical clusters with particle size less than 15 nm. The FT-IR spectra suggested the complexation between β-CD and Ag-Cts and the stability was assessed by Zeta potential measurement. Obtained zones of MIC for gram positive and gram negative bacteria suggest that the β-CD stabilized Ag-Cts NC is a promising antibacterial agent.

Acknowledgements

Thanks are due to our mentors and Mr. R. Mohan for their helpful discussion. The author would like to acknowledge Manonmaniam Sundaranar University, Annamalai University for SEM, AFM, XRD, FT-IR & UV–Visible spectral analysis and also Anna University for timely recording of HR-TEM.

References

[1] P. Grodzinski, M. Silver, L.K. Molnar, Expert Rev. Mol. Diagn. 6 (2006) 307–318.
[2] W. Cai, X. Chen, Small 3 (2007) 1840–1854.
[3] W. Cai, X. Chen, J. Nucl. Med. 49 (2008) 113S–128S.
[4] V. Polshettiwar, R.S. Varma, Green Chem. 12 (2010) 743–754.
[5] T. Yang, Z. Li, L. Wang, C. Guo, Y. Sun, Langmuir 23 (2007) 10533–10538.
[6] A. Rangnekar, T.K. Sarma, A.K. Singh, J. Deka, A. Ramesh, A. Chattopadhyay, Langmuir 23 (2007) 5700–5706.
[7] S. Naraginiti, A. Sivakumar, Spectrochim. Acta A 128 (2014) 357–362.
[8] A. Lalitha, R. Subbaiya, P. Ponmurugan, Int. J. Curr. Microbiol. Appl. Sci. 2 (6) (2013) 228–235.
[9] M.F. Zayed, W.H. Eisa, A.A. Shabaka, Spectrochim. Acta A 98 (2012) 423–428.
[10] P. Raveenderan, J. Fu, S.L. Wallen, J. Am. Chem. Soc. 125 (2003) 13940–13941.
[11] D.K. Bozanic, V. Djokovic, J. Blanuša, P.S. Nair, M.K. Georges, T. Radhakrishnan, Eur. Phys. J.E 22 (2007) 51–59.
[12] A. Pal, K. Esumi, T. Pal, J. Colloid Interface Sci. 288 (2005) 396–401.
[13] R. Brayner, M.J. Vaulay, F. Fievet, T. Coradin, Chem. Mater. 19 (2007) 1190–1198.
[14] C.M. Shih, Y.T. Shieh, Y.K. Twu, Carbohydr. Polym. 78 (2009) 309–315.
[15] A. Murugadoss, A. Chattopadhyay, Nanotechnology 19 (2008) 015603.
[16] D.K. Bozanic, L.V. Trandafilovic, A.S. Luyt, V. Djokovic, React. Funct. Polym. 70 (2010) 869–873.
[17] C.M. Sun, R.J. Qu, H. Chen, C.N. Ji, C.H. Wang, Y.Z. Sun, B.H. Wang, Carbohydr. Res. 343 (2008) 2595–2599.
[18] D.W. Wei, W.P. Qian, Colloids Surf. B 62 (2008) 136–142.
[19] V.K. Sharma, R.A. Yngard, Y. Lin, Adv. Colloid Interf. Sci. 145 (2009) 83–96.
[20] K. Aslan, J. Zhang, J.R. Lakowicz, C.D. Geddes, J. Fluoresc. 14 (2004) 391–400.
[21] A. Vaseashta, D. Dimova-Malinovska, Sci. Technol. Adv. Mater. 6 (2005) 312–318.
[22] S.R. Nicewarner-Pena, R.G. Freeman, B.D. Reiss, L. He, D.J. Pena, I.D. Walton, R. Cromer, C.D. Keating, M.J. Natan, Science 294 (2001) 137–141.
[23] H.F. Salem, K.A.M. Eid, M.A. Sharaf, Int. J. Drug Delivery 3 (2011) 293–304.
[24] M.I. Sriram, S.B. Mani Kanth, K. Kalishwaralal, S. Gurunathan, Int. J. Nanomed. 5 (2010) 753–762.
[25] V. Kathiravan, S. Ravi, S. Ashokkumar, Spectrochim. Acta A 130 (2014) 116–121.
[26] M. Rai, A. Yadav, A. Gade, Biotechnol. Adv. 27 (2009) 76–83.
[27] R. Vaidyanathan, K. Kalishwaralal, S. Gopalram, S. Gurunathan, J. Bio. Technol. Adv. 27 (2009) 924–937.
[28] C. Baker, A. Pradhan, L. Pakstis, D.J. Pochan, S.I. Shah, J. Nanosci. Nanotechnol. 5 (2005) 244–249.
[29] B.U. Lee, S.H. Yun, J.H. Ji, G.N. Bae, J. Microbiol. Biotechnol. 18 (2008) 176–182.
[30] K.H. Cho, J.E. Park, J. Osaka, S.G. Park, Electrochim. Acta 51 (2005) 956–960.
[31] J. Liu, W. Ong, E. Roman, M.J. Lynn, A.E. Kaifer, J. Langmuir. 16 (2000) 3000–3002.
[32] B. He, J.J. Tan, K.Y. Liew, H.J. Liu, Mol. Catal. A Chem. 221 (2004) 121–126.
[33] S. Giuffrida, G. Ventimiglia, S. Petralia, S. Conoci, S. Sortino, Inorg. Chem. 45 (2006) 508–510.
[34] J. Alvarez, J. Liu, E. Roman, A.E. Kaifer, Chem. Commun. 8 (2000) 1151–1152.
[35] J. Liu, J. Alvarez, W. Ong, E. Roman, A.E. Kaifer, J. Am. Chem. Soc. 123 (2001) 11148–11154.
[36] Y. Liu, K.B. Male, P. Bouvrette, J.H.T. Luong, Chem. Mater. 15 (2003) 4172–4180.
[37] S. Panigrahi, S. Nath, S. Praharaj, S.K. Ghosh, S. Kundu, S. Basu, T. Pal, Colloids Surf. A Physicochem. Eng. Aspects 264 (2005) 133–138.
[38] S. Pande, S.K. Ghosh, S. Praharaj, P. Suldipa, S. Basu, S. Jana, A. Pal, T. Tsukuda, T. Pal, J. Phys. Chem. 111 (2007) 10806–10813.
[39] R.G. Puspha, A.G. Annaselvi, P. Subramaniam, Int. J. Nanomat. Biost. 3 (1) (2013) 26–30.
[40] Z. Karim, R. Adnan, Arch. Environ. Sci 6 (2012) 1–12.
[41] K.L. Kelly, E. Coronado, L.L. Zhao, G.C. Schatz, J. Phys. Chem. B 107 (2003) 668–677.
[42] A.L. Stepanov, J. Technical. Phys. 49 (1997) 143–153.
[43] K.G. Stamplecoskie, J.C. Scaiano, J. Am. Chem. Soc. 132 (2010) 1825–1827.
[44] N.F. Mott, E.A. Davies, Electronic Processes in Non-Crystalline Materials, second ed., Clare don Press, Oxford, 1979.
[45] H. Kumar, R. Rani, Int. J. Eng. Innovative Technol. 3 (2013) 344–348.
[46] A.N. Banerjee, K.K. Chattopadhyay, D. Depla, S. Maheiu (Eds.), Springer– Verlag, Berlin, Heidelberg, 2008.
[47] M. Zargar, A.A. Hamid, F.B. Bakar, M.N. Shamsudin, K. Shameli, F. Jahanshiri, F. Farahani, J. Mol. 16 (2010) 6667–6676.
[48] K. Raja, P.S. Ramesh, D. Geetha, Spectrochim. Acta A 120 (2013) 19–24.
[49] K. Mallikarjuna, G. Narasimha, G.R. Dillip, B. Praveen, B. Shreedhar, C. Sree Lakshmi, B.V.S. Reddy, B. Deva Prasad Raju, Digest J. Nanometer Biostruct. 6 (2011) 181–186.

[50] G. Saraswathy, S. Pal, C. Rose, T.P. Sastry, Bull. Mater Sci. 24 (2001) 415–420.
[51] S. Wazed Ali, S. Rajendran, M. Joshi, Carbohydr. Polym. 83 (2001) 438–446.
[52] P. Gupta, M. Bajpai, S.K. Bajpai, J. Cotton Sci. 12 (2008) 280–286.
[53] M. Beltramini, K. Lerch, Neurospora tyrosinase: intrinsic and extrinsic fluorescence, in: I. Bertini, R.S. Drago, C. Luchinat Kluwer (Eds.), The Coordination Chemistry of Metalloenzymes, Boston, 1982, p. 236.
[54] S. Govindan, E.A.K. Nivethaa, R. Saravanan, V. Narayanan, A. Stephen, Appl. Nanosci. 2 (2012) 299–303.
[55] K. Gupta, P.C. Jana, A.K. Meikap, Synth. Met. 160 (2010) 1566–1573.
[56] D.W. Tang, S.H. Yu, Y.C. Ho, F.L. Mi, P.L. Kuo, H.W. Sung, Biomaterials 31 (2010) 9320–9332.
[57] X.L. Cao, C. Cheng, Y.L. Ma, C.S. Zhao, Mater. Sci.: Mater. Med. 21 (2010) 2861–2868.
[58] J.R. Morones, J.L. Elechiguerra, A. Camacho, K. Holt, J.B. Kouri, J.T. Ramírez, Nanotechnology 16 (2005) 2346–2353.